



ELSEVIER

Contents lists available at ScienceDirect

Organic Electronics

journal homepage: www.elsevier.com/locate/orgel

Meyer–Neldel rule for charge carrier transport in fullerene devices: A comparative study

A. Pivrikas^{a,*}, Mujeeb Ullah^b, Th.B. Singh^a, C. Simbrunner^b, G. Matt^a, H. Sitter^b, N.S. Sariciftci^a

^a Linz Institute for Organic Solar Cells (LIOS), Physical Chemistry, Johannes Kepler University, Altenberger Str. 69, A-4040 Linz, Austria

^b Institute of Semiconductor and Solid State Physics, Johannes Kepler University, Altenberger Str. 69, A-4040 Linz, Austria

ARTICLE INFO

Article history:

Received 21 May 2010

Received in revised form 21 October 2010

Accepted 21 October 2010

Available online 12 November 2010

Keywords:

Meyer–Neldel rule

Arrhenius

CELIV

OFET

Carrier mobility

Charge transport

ABSTRACT

Charge transport is comparatively studied in the bulk and at the interface of disordered fullerene films fabricated using physical vapour deposition. Charge carrier concentration and temperature dependent electron mobilities are comparatively studied using charge extraction by linearly increasing voltage (CELIV) technique and organic field-effect transistors (OFET) measurements. Electron mobility is at least two orders of magnitude higher than hole mobility in the fullerene films. Lower mobility values and stronger concentration dependence in diodes is observed. Carrier concentration dependent activation energy is experimentally measured in both types of devices. Larger activation energy for electron transport is required at lower carrier concentrations. Meyer–Neldel rule (MNR) for electron mobility is observed in both the bulk of the fullerene films and in the transistor channel at the interface. Meyer–Neldel energy ($E_{MN} = 35$ meV), which is interpreted as disorder parameter, is the same in both device geometries, which suggest that the level of disorder and energetical landscape for charge transport is similar in the bulk of fullerene films and at the interface with the insulator. Disorder formalism is used to qualitatively explain that either carrier concentration or the nature of non-equilibrium charge carrier transport in CELIV compared to steady-state OFET measurements is responsible for observed transport properties.

© 2010 Elsevier B.V. All rights reserved.

1. Introduction

The charge carrier transport mechanisms are fundamentally important for understanding the electronic phenomena in organic semiconductor devices. In general, charge carrier transport is dependent on the material structure and nanoscale order in the film [1]. One of the advantages of organic electronic devices is their solution processability, which results in disordered film structures. The absence of translational symmetry with a three-dimensional periodic lattice in disordered films results in a random distribution of potential wells yielding a distribution of localized density of states (DOS). Hopping type of charge transport leads to a lower carrier mobility compared to crystalline inorganic semiconductors. Charge

carrier transport studies in disordered organic semiconductors are challenging due to low charge carrier mobility ($<1 \text{ cm}^2 \text{ V}^{-1} \text{ s}^{-1}$) (limits the applicability of Hall effect), a significant amount of thermally generated carriers (limits the applicability of time-of-flight – TOF), pronounced trapping, dispersive transport, non-Ohmic contacts (limits the applicability of space charge limited current – SCLC) makes the standard measurement methods difficult to apply [2–7].

Various physical processes, including charge carrier transport in disordered media, are thermally activated and follow the Arrhenius exponential law of the form [8]:

$$\mu = \mu_0 \exp\left(-\frac{E_A}{kT}\right), \quad (1)$$

where k is the Boltzmann constant, T is the temperature, μ_0 is the prefactor and E_A is the activation energy. Meyer and

* Corresponding author.

E-mail address: almantas.pivrikas@jku.at (A. Pivrikas).

Neldel first observed the exponential dependence of the prefactor μ_0 on the activation energy E_A :

$$\mu_0 = \mu_{MN} \exp\left(\frac{E_A}{kT_{MN}}\right), \quad (2)$$

where μ_{MN} is the Meyer–Neldel mobility and $kT_{MN} = E_{MN}$ is the Meyer–Neldel energy. Substituting Eq. (2) into Eq. (1) leads to the consequence that there exist an isokinetic temperature $T = T_{MN}$, where the charge carrier mobility becomes independent on activation energy E_A . In a plot of $\ln(\mu)$ versus the inverse temperature (Arrhenius plot), the lines of different Arrhenius dependencies should show one common intersection at T_{MN} . Charge carrier concentration is a parameter which changes the activation energy in MNR. During the transport, the charge carriers become de-trapped by being excited from localized states to extended states (or to the states with higher energies where density of states is higher if delocalized states do not exist) by acquiring thermal energy (Arrhenius type behaviour) [9]. Carrier concentrations determines the occupation of DOS as well as the activation energy required for carriers to acquire in order to be promoted to states with higher mobility. Therefore, higher carrier mobility is expected at high concentrations.

The Meyer–Neldel rule (MNR) was observed in charge carrier mobility of fullerenes [10], porous and amorphous silicon [11], microcrystalline silicon films [12], ionic conductivity [13] glassy materials [14] organic materials [15] in various devices such as charge-coupled devices [16], liquid semiconductors [17] and thin-film transistors [18]. Meyer–Neldel temperature was even attributed as a figure-of-merit for the quality of materials used in field-effect transistors [19]. Even though a number of theoretical models were proposed to explain the origin of MNR, none of them is universally accepted. One common explanation is based on the Fermi level shift with temperature [20]. Others suggest that MNR arises for processes for which the total energy is provided by multiple excitations [21,22]. It was also shown that multiple processes coexisting at the same time also lead to the MNR [23]. Theoretical studies by Fishchuk et al., proposed this Meyer–Neldel energy kT_{MN} to be directly proportional to the width of the DOS in the disordered energy band [24].

Usually electric current, conductivity, diffusion and other physical parameters are used to determine the presence of MNR. In order to clearly understand the mechanisms of MNR it is important to demonstrate the MNR in fundamental quantities such as charge carrier mobility. Other quantities might depend on non-transport parameters, for instance material conductivity or total current are dependent on both charge carrier mobility and density which hinders the interpretation of experimental results.

In order to understand and be able to develop device independent unifying models of charge transport it is important to study transport in various device configurations. A number of studies have comparatively studied the charge transport using TOF and OFETs in the past [25–28]. The charge carrier mobility as a function of carrier concentration and temperature is comparatively studied in the bulk of fullerene (C_{60}) diodes and at the interface with

gate insulators in OFETs. Usually a large discrepancy between the bulk and the interface mobility values is observed, which is attributed to the difference in charge carrier concentrations and to the difference of the DOS at the interface and in the volume of the film [29,30].

Due to the possibility to experimentally vary carrier concentration and temperature, charge extraction with linearly increasing voltage (CELIV) technique and organic field effect transistor (OFET) measurements are advantageous for studying the charge carrier transport, whereas carrier concentration cannot be varied in classical time-of-flight technique. However, non-equilibrium transport of photogenerated charge carriers is studied using CELIV, whereas steady-state transport is measured in OFETs. Photogenerated carriers lose their excess energy during thermalization processes (downward jumps in energy scale) and their mobility decreases with time after photogeneration resulting in a time-dependent dispersive transport [31]. Therefore, when comparing photogenerated with steady-state transport this has to be taken into account.

In this work the charge carrier mobility as a function of carrier concentration and temperature is studied in fullerene (C_{60}) diodes and OFETs. Comparative studies of charge transport in the bulk of the film and at the interface of fullerene and dielectric are reported using CELIV as well as OFET techniques. MNR parameters have been used to determine the quality of the films and the degree of disorder [19]. Activation energy of electron transport is experimentally measured as a function of carrier concentration.

2. Experimental

The schematic structures of the devices studied here are shown in Fig. 1. Diodes are made of sandwich type geometry, where the semiconducting film is placed between aluminum and PEDOT covered ITO electrodes. OFETs are planar contacted structures where charge carrier transport proceeds between the source and drain electrodes within the channel at the interface of the semiconductor and insulator.

2.1. Charge carrier mobility measurements by charge extraction by linearly increasing voltage (CELIV)

CELIV allows the charge carrier mobility and concentration to be measured from current transients directly and independently. Moreover, time, density, electric field and temperature dependent charge carrier mobility can be studied in the films with rather dispersive charge transport, where other methods (e.g. time-of-flight) are inapplicable due to required experimental conditions [2]. It was shown in the past that the charge carrier mobility measured from CELIV is in good agreement with values measured by TOF [32]. Schematic time dependence of the applied triangle rising voltage pulse and current transient response is shown in Fig. 2.

A linearly increasing voltage pulse with the slope $A = U_{\max}/t_{\text{pulse}}$, here U_{\max} is the maximum voltage of triangle pulse and t_{pulse} is the pulse duration) is applied to the sample to extract the equilibrium charge carriers. The

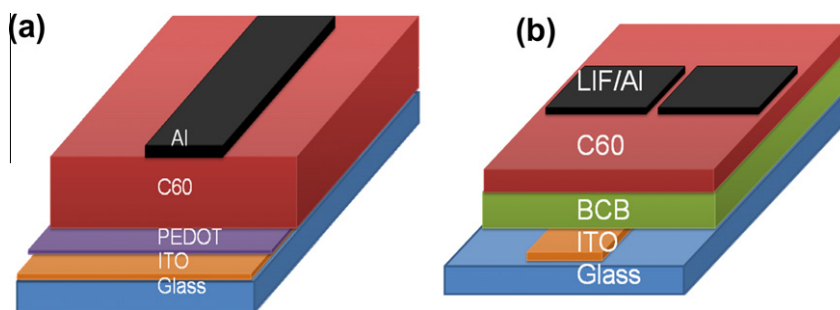


Fig. 1. Schematic illustration of diodes (a) for CELIV and organic field effect transistor (b) for OFET structures used to comparatively study the charge carrier transport in the bulk of the C₆₀ film (between Al and ITO/PEDOT contacts) and at the interface of fullerene with the gate insulator (between LiF/Al contacts but at the C₆₀/insulator (BCB) interface).

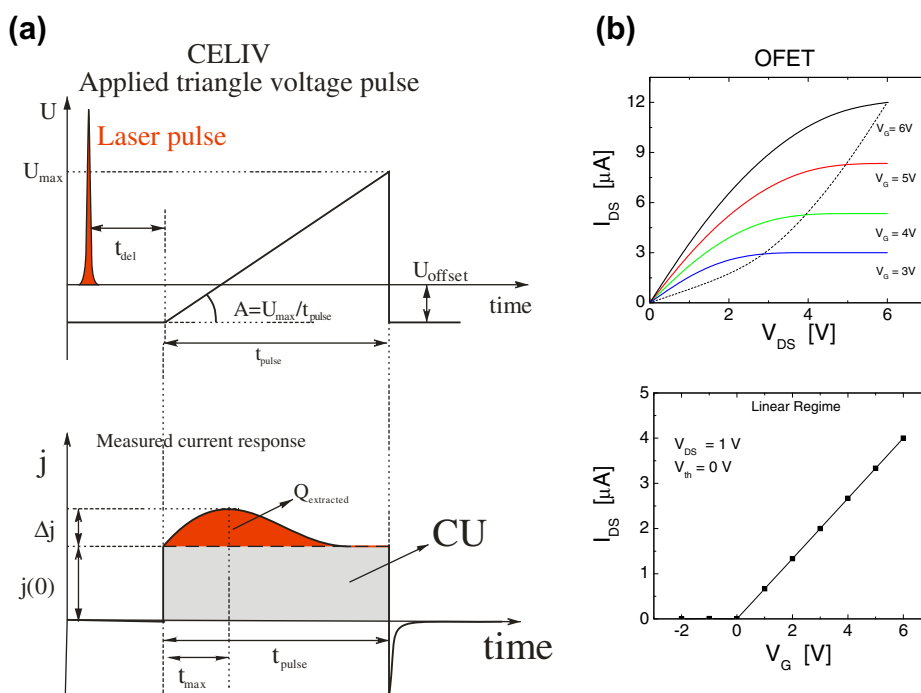


Fig. 2. Schematic charge extraction by linearly increasing voltage (CELIV) current transients (a) and organic field effect transistor (FET) output and transfer curves (b) used to experimentally measure the charge carrier mobility. The charge carrier mobility was studied as a function of the following parameters: temperature, time t_{del} from CELIV, electric field (by changing the rising slope of triangle voltage pulse in CELIV and drain-source voltage V_{DS} in OFET), charge carrier concentration (by changing t_{del} and measuring extracted charge $Q_{\text{extracted}}$ in CELIV and changing V_{G} in OFET).

charge carriers inside the film can also be photogenerated by a light pulse (sometimes called photo-CELIV technique, herein referred also as CELIV). Then, the photogenerated charge carriers are extracted by the linearly increasing voltage pulse after some delay time t_{del} . At the beginning of the CELIV current transient a capacitive current step $j(0)$ is seen (Fig. 2a). The following current increase Δj is related to the extraction current caused by the charge carriers transported in the film. The current continues to increase as the voltage increases until the charge carriers are extracted from the film and the current drops down to the capacitive step level. In practice, if the duration of the applied triangle voltage pulse t_{pulse} is not long enough, then there might be some carriers left in the film and the extraction current will end at a higher level than the

capacitive step. The charge carrier mobility is estimated from the extraction maximum [33]:

$$\mu = K \frac{d^2}{At_{\text{max}}^2}, \quad (3)$$

where d is the film thickness, $K = 2/3$ for volume ($\alpha d \ll 1$, where α is light absorption coefficient from Beer–Lambert’s law) and $K = 2$ for surface photogeneration ($\alpha d \gg 1$).

The charge carrier concentration ($n = Q_{\text{extracted}}/eV$, where $Q_{\text{extracted}}$ is the extracted charge, e the elementary charge and V is the volume) is estimated from the integrated extraction photocurrent transient with respect to time. By changing the delay time (t_{del}) between the laser pulse and applied voltage pulse, or by changing the laser

intensity, the charge carrier mobility was measured as a function of time and concentration [34]. Since the electrical field in CELIV experiments is not a constant value but it is ramping with time, the field at which the charge carrier mobility is measured is estimated from At_{\max}/d (electric field at maximum extraction point t_{\max}), since majority of carriers are extracted at this field.

Thick fullerene films ($\approx 1\text{--}10\ \mu\text{m}$, in order to ensure surface photogeneration) were grown on ITO/glass substrates using physical vapor deposition [35]. Semitransparent, 30 nm thick aluminum electrode was vacuum deposited on top of the fullerene films. CELIV could only be measured down to 240 K in due to a phase transition and a peel off of the studied films. In both, CELIV and OFET experiments, the charge carrier mobility and its temperature dependencies were measured in a cryostat under vacuum (10^{-6} mbar). The measurements were conducted with a temperature step of 10 K, with a time delay of 1 h so that device got thermally stabilized. Studied devices were loaded in the Oxford cryostat under N_2 atmosphere inside the glove box to avoid exposure to ambient condition.

2.2. Charge carrier mobility measurements by organic field effect transistor (OFET)

Fig. 2 shows typical output characteristics of a FET device at different gate voltages and the corresponding transfer characteristics in the linear regime ($V_G \gg V_{DS}$, where V_G and V_{DS} are the gate and drain-source voltages correspondingly). In linear regime, the applied gate field is much larger than the in-plane drift field, which results in an approximately uniform density of charge carriers in the active channel. At these conditions source-drain current I_D increases linearly with V_G and is approximately described by the following equation:

$$I_D|_{V_{DS} \ll V_G} = \frac{W}{L} \mu C_i V_{DS} (V_G - V_{th}) \quad (4)$$

where L is the channel length, W is the channel width, C_i is the capacitance per unit area of the insulating layer, V_{th} is the threshold voltage.

By plotting I_D versus V_G at low V_{DS} and evaluating the slope of this plot, the carrier mobility μ can be calculated using Eq. (4). Similarly, mobility can also be determined in the saturation regime ($V_{DS} \geq V_G$), but due to pinch off in the channel, the mobility calculated in the saturated regime is not an option to study the charge carrier transport in FET devices, because it is deduced from an inhomogeneous distribution of the charge carriers in the conductive channel of the FET.

The charge carrier concentration n is estimated from the charge accumulated at the semiconductor/insulator interface by increasing V_G in metal-insulator-semiconductor (MIS) capacitor:

$$n = C_i V_G \frac{1}{ed}, \quad (5)$$

where e is the elementary charge, C_i is the geometric capacitance of the device with a 35 μm channel length and 2 mm channel width and d is the channel height.

Since the charge carrier transport is strongly dependent on the insulator and interface/surface treatment in OFETs [36], OFET devices were fabricated using inert divinyltetramethyldisiloxane-bis(benzocyclobutene) (BCB) as gate dielectric on ITO/glass substrates. Transistor channel length was 35 μm , width 2 mm and for concentration calculations we assumed the channel thickness on the interface of 10 nm (where most of the charge carriers are accumulated) [37]. Details of device fabrication steps were reported previously [38]. The transistor characteristics were recorded by Agilent 2000 SMU. Low V_{DS} (2, 4, 6, 8, 10 V) compared to high V_G (60 V) was used in the experiment in order to stay in the linear regime of OFET operation.

3. Results and discussion

In order to determine the charge transport properties of the studied C_{60} films, both CELIV and OFET measurements were employed. In order to compare the electron and hole mobility by CELIV, thick fullerene films were illuminated either through semitransparent Al or ITO electrode keeping the same applied voltage polarity [39]. Therefore, either electron (ITO illuminated with negative bias) or hole (Al illuminated with positive bias) transport can be measured in the film where the light absorption profile is much smaller than film thickness (surface photogeneration).

Fig. 3a shows CELIV transients for electron and hole transport. The extraction current is seen only for electron transport, whereas for hole transport the CELIV transients is indistinguishable with the dark response concluding that the electron mobility is much higher (>100 times) compared to hole mobility. Laser signal is well seen before the extraction pulse showing that the electrons and holes are photogenerated at the aluminum interface.

The current response for electron transport resembles a typical CELIV transient. The capacitive (displacement) charging current for dark transients is slightly increasing with time due to sum of both effects: increasing dielectric constant and carrier injection from electrode due to non-perfectly blocking contacts. Extraction maximum is seen only for electron transport, when negatively biased ITO electrode is illuminated with a laser.

The OFET transfer curve, shown in Fig. 3b, shows no significant hole injection into the channel when negative voltage is applied to the gate. Strong electron current is observed under positive gate bias. Therefore, both CELIV and OFET experiments confirm that electron mobility is much higher than hole in fullerene films. Further charge carrier transport studies in this work are shown for electron mobility.

Carrier mobility measurements as a function of carrier concentration at various temperatures is shown Fig. 4. In CELIV experiment (a) and (b) the transients were recorded at different t_{del} . The triangle voltage slope A was fixed, but the delay time between the laser and voltage pulse t_{del} was varied which changed carrier concentration. In OFET experiment (c) and (d) the transfer curves at different gate voltages are shown.

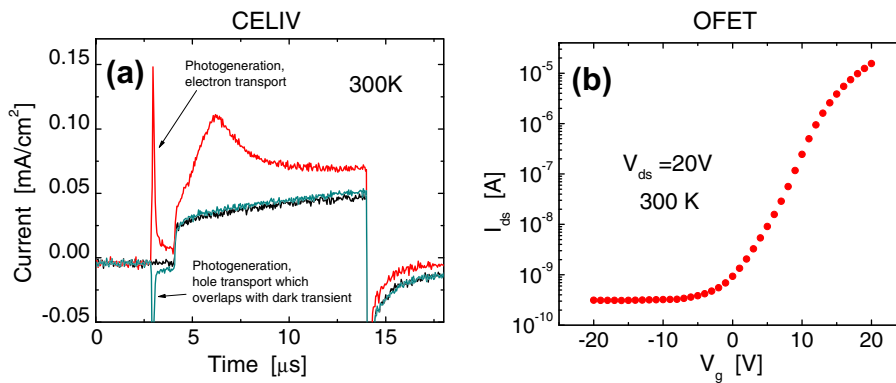


Fig. 3. CELIV transients (a) and OFET transfer curve (b) showing that the electron mobility is at least 100 times larger than hole mobility in C_{60} .

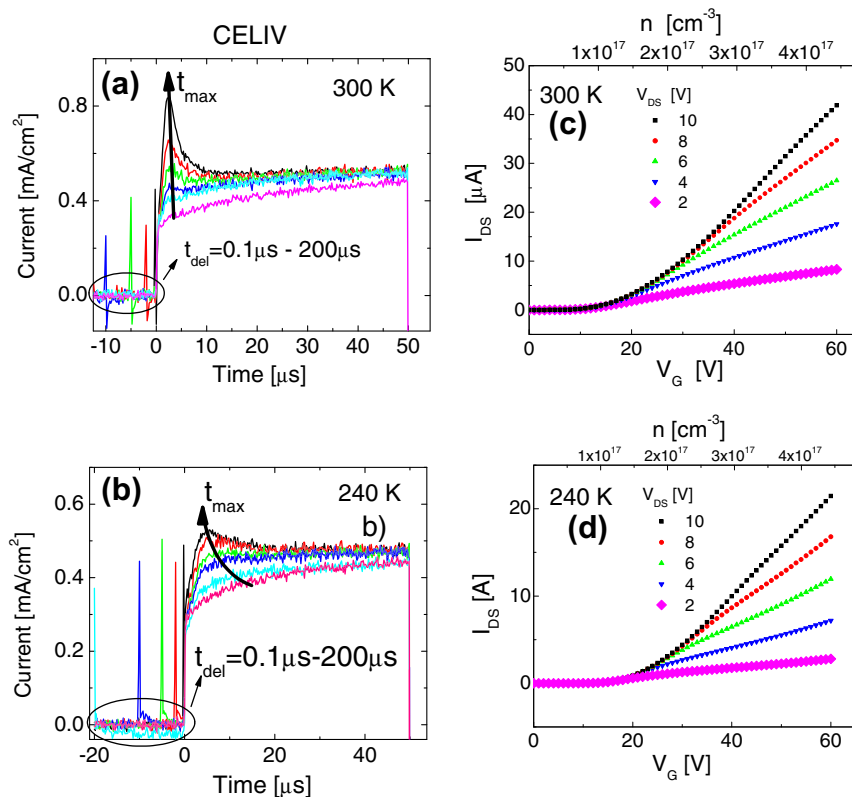


Fig. 4. CELIV current transients at various delay times t_{del} in (a) and (b) shown together with OFET transfer curves in (c) and (d) both at 300 K and 240 K, respectively. From CELIV transient time and concentration dependent carrier mobility as well as carrier density relaxation is measured. OFET curves (shown as thick points) are used to measure carrier concentration dependent electron mobility at different gate voltages.

CELIV transients are similar to the ones observed before only showing more dispersive extraction at lower temperatures. Stronger shift in extraction maximum, which is related to carrier mobility, can be seen at lower temperatures, directly showing that stronger concentration dependent carrier mobility at low temperatures. Charge carrier mobility dependence on time is calculated using Eq. (3) and plotted in Fig. 5a. Because the carrier

extraction is not instantaneous and t_{max} is comparable delay time t_{del} , both times have to be taken into account. Therefore, the sum of t_{del} and t_{max} is plotted in Fig. 5 [40].

The charge carrier mobility decreases as a function of time due to the relaxation phenomena of photogenerated charge carriers (thermalization) within the density-of-states to deeper states (time-dependent mobility) as well as due to the charge carrier recombination during the de-

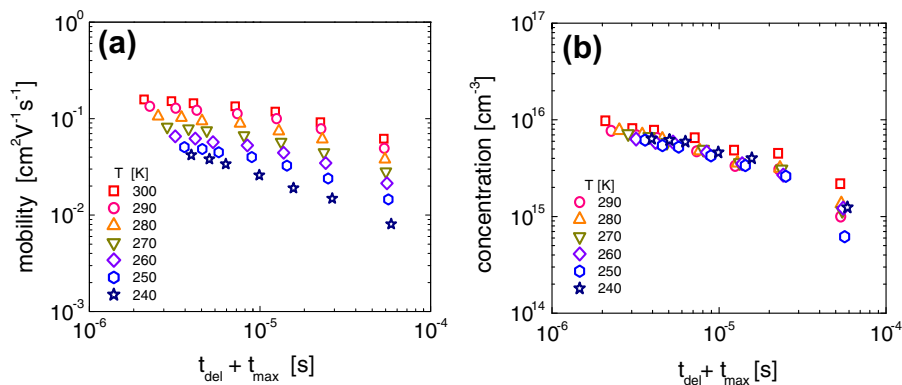


Fig. 5. Non-equilibrium time-dependent electron mobility (a) and density decay (b) in C60 films shown at various temperatures as measured from CELIV.

lay time t_{del} (concentration-dependent mobility) [40]. In the studied films charge transport is weakly dispersive especially at room temperatures, therefore only weak carrier mobility dependence on time is seen. Therefore, measured mobility dependence is attributed to carrier concentration.

By integrating the extraction photocurrent (dark current subtracted) of the CELIV transient over time, we estimate the amount of extracted charge which is proportional to charge carrier concentration in the film. Time-resolved decay of charge carrier concentration is measured and plotted in Fig. 5b. Charge carrier concentration is similar at all temperatures showing that appropriate experimental conditions were chosen to extract all photogenerated charge carriers which allow carrier concentration to be estimated from the photocurrent transients. In order to present the carrier mobility as a function of concentration, Fig. 5a and b are used to eliminate the time scale and plot carrier mobility at different concentrations. Carrier mobility values from OFET are estimated from Fig. 4 using Eq. (4) and plotted together with CELIV values comparatively in Fig. 6. Since the extraction maximum position changes with carrier concentration, so does the electric field at

which carrier mobility is estimated. Therefore, non-constant electric field is present during CELIV measurements, but the change is insignificant (from 3000 to 1500 V/cm), whereas in OFET experiment the electric field is constant (500 V/cm).

Much lower charge carrier mobility values and stronger concentration dependence is seen in the bulk of the film from CELIV where carrier concentration is significantly lower. Weak dependence of carrier mobility on concentration observed in OFETs is attributed to the trap filling effect at high carrier concentrations which increases the effective transport energy in the DOS to higher values. This allows for carriers to reach higher energies where the mobility is larger and less dependent of concentration due to higher density of available states [41].

Arrhenius plots from both CELIV and OFET experiments are evaluated from the concentration dependent carrier mobility measurements. Fig. 7a and b shows the Arrhenius-type of charge carrier mobility replotted from the Fig. 6 as a function of temperature at different carrier concentrations from both CELIV and OFET experiments, respectively.

In both experiments carrier mobility follows Arrhenius type of dependence in contrast to typically observed non-Arrhenius dependence in π -conjugated polymers and molecularly doped polymer in which Bässler's model is used to describe the charge transport.[32,41] A common intersection point of extrapolated data lines allows the Meyer–Neldel parameters to be estimated. The charge carrier mobility becomes temperature and concentration independent at the isokinetic intersection point. MNR temperature obtained from CELIV is $T_{\text{MN}} = 406$ K and from OFET $T_{\text{MN}} = 408$ K which in both cases corresponds approximately to $E_{\text{MN}} = 35$ meV. Since the MNR energy E_{MN} is directly correlated with the level of disorder in the film quality and properties of DOS in which charge transport occurs [24,42,43], similar MNR energies obtained from CELIV and OFET suggest that charge carriers experience energetically similar landscape for charge transport in the bulk of the film and at the interface in studied devices. The absence of dipoles at the interface of fullerene and BCB forms the interface beneficial for charge transport which allows to reach high carrier mobility values. The MNR mobility

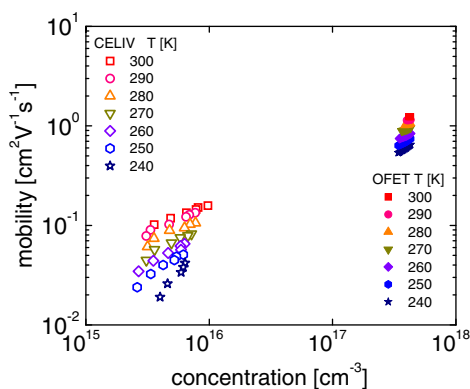


Fig. 6. Concentration dependent electron mobility in C₆₀ films measured from CELIV and OFET. Electric field in CELIV experiment changes in the range from 3000 to 1500 V/cm, where in OFETs it is 500 V/cm.

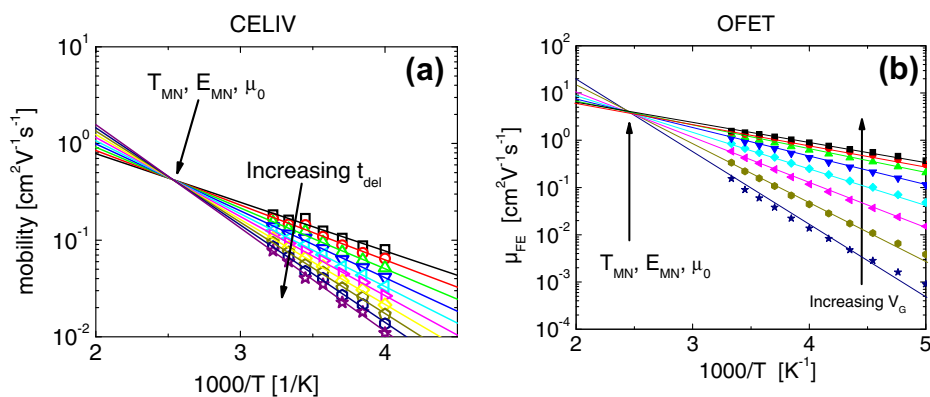


Fig. 7. Arrhenius plots of temperature dependent electron mobility at various concentrations measured from CELIV and OFET. Meyer-Neldel parameters from CELIV: $T_{MN} = 406$ K, $E_{MN} = 35$ meV, $\mu_{MN} = 0.4$ cm² V⁻¹ s⁻¹; from OFET: $T_{MN} = 408$ K, $E_{MN} = 35$ meV, $\mu_{MN} = 4$ cm² V⁻¹ s⁻¹.

prefactors (Eq. (2)) are $\mu_{MN} = 0.4$ cm² V⁻¹ s⁻¹ from CELIV and $\mu_{MN} = 4$ cm² V⁻¹ s⁻¹ from OFET. Obtained values are in good agreement with the results obtained in similar C₆₀ devices in the past [10,24,42,43].

From Arrhenius plots the activation energies for electron transport are estimated from both CELIV and OFET measurements and plotted as a function of carrier concentration in Fig. 8a. Electric field at which concentration dependent carrier mobility was measured is different in both experiments. High voltage was used in CELIV to ensure the lowest error, whereas to satisfy linear regime conditions in OFET measurements, the smallest source-drain voltage was used. Despite a slight mismatch observed in Fig. 8a, the correct trend of activation energy is seen. At lower carrier concentrations larger activation energy is required for transport in disordered media.

We have estimated and plotted in Fig. 8b the mobility prefactor μ_0 as a function of activation energy using Eq. (1). Similar slopes show well matching MNR energies E_{MN} in both the bulk on the film and at the interface. The mobility prefactor μ_0 is order of magnitude higher in the OFET compared to transport in the bulk measured from CELIV, which well agrees with the difference in Meyer–Neldel mobility prefactor μ_{MN} as well as with difference in activation energies E_A .

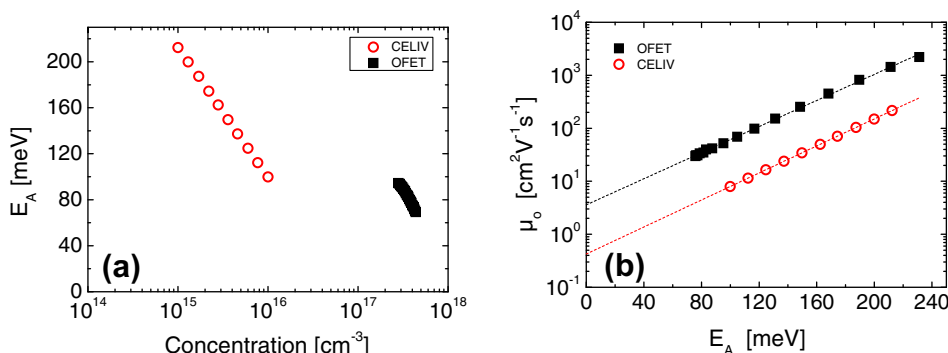


Fig. 8. (a) activation energy dependence on concentration. Electric field changes in the same range as specified in the caption of Fig. 6; (b) mobility prefactor μ_0 dependence on activation energy E_A shown for CELIV and OFET experiments.

A mismatch in μ_{MN} , μ_0 and E_A in diodes and OFETs can be caused by the nature of non-equilibrium measurements in CELIV compared to steady-state OFET measurements. Excess amount of energy available for photogenerated charge carriers might reduce the activation energy and be the reason for the observed mismatch. Further studies of concentration dependent activation energy at different electric fields is required in order to see the effect of electric field.

4. Conclusions

Carrier density and temperature dependent mobility is experimentally measured and compared in the bulk of the fullerene films and at the interface with insulator. Non-equilibrium mobility of photogenerated charge carriers measured using charge extraction by linearly increasing voltage (CELIV) technique as well as steady state mobility measured in organic field-effect transistors (OFET) is compared. Much higher electron mobilities (>100 times) as compared to hole mobilities are observed. Carrier concentration dependent electron mobility in both types of devices shows lower mobility values and stronger concentration dependence in diodes. Larger activation energy for electron transport is required at lower carrier

concentrations. Arrhenius plots of temperature dependence of mobility at various concentrations demonstrate the presence of Meyer–Neldel rule (MNR). It is shown that MNR energy is the same in the bulk of the semiconductor and at the interface, suggesting similar levels of energetical disorder. Observed differences in charge transport in diodes and OFETs is proposed to be due to either different carrier concentrations or due to the nature of non-equilibrium charge carrier transport in CELIV compared to steady-state OFET measurements.

Acknowledgements

We thank Prof. I.I. Fishchuk and Prof. A.K. Kadashchuk for helpful scientific discussions. Austrian National Network (NFN S9711) funded by the Austrian Science Funds (FWF) is acknowledged.

References

- [1] Paul M. Borsenberger, *Mol. Cryst. Liquid Cryst.* 228 (1993) 167.
- [2] G. Juska, K. Genevicius, K. Arlauskas, R. Osterbacka, H. Stubb, *Phys. Rev. B* 65 (2002) 233208.
- [3] A. Pivrikas, G. Juska, K. Arlauskas, M. Scharber, A. Mozer, N.S. Sariciftci, H. Stubb, R. Osterbacka, *Proc. SPIE* 5938 (2005) 59380N.
- [4] G. Juška, G. Sliuzys, K. Genevicius, K. Arlauskas, A. Pivrikas, M. Scharber, G. Dennler, N.S. Sariciftci, R. Osterbacka, *Phys. Rev. B* 74 (2006) 115314.
- [5] G. Juška, K. Arlauskas, G. Sliuzys, A. Pivrikas, A.J. Mozer, N.S. Sariciftci, M. Scharber, R. Osterbacka, *Appl. Phys. Lett.* 87 (2005) 222110.
- [6] G. Juška, K. Genevicius, G. Sliuzys, A. Pivrikas, M. Scharber, R. Osterbacka, *J. Appl. Phys.* 101 (2007) 114505.
- [7] R. Osterbacka, K. Genevicius, A. Pivrikas, G. Juška, K. Arlauskas, T. Kreuzis, D.D.C. Bradley, H. Stubb, *Synth. Met.* 139 (2003) 811.
- [8] W. Meyer, H. Neldel, *Z. Tech. Phys. (Leipzig)* 12 (1937) 588.
- [9] P.W. Anderson, Absence of diffusion in certain random lattices, *Phys. Rev.* 109 (1958) 1492–1505.
- [10] J.C. Wang, Y.F. Chen, *Appl. Phys. Lett.* 73 (1998) 948.
- [11] Y. Lubianiker, I. Balberg, *J. Non-Crystalline Solids* 227–230 (1998) 180.
- [12] S.K. Ram, S. Kumar, R. Vanderhaghen, P. Roca i Cabarrocas, *J. Non-Crystalline Solids* 411 (2002) 299–302.
- [13] K.L. Ngai, *Sol. Stat. Ionics* 105 (1998) 231.
- [14] K. Shimakawa, F. Abdel-Wahab, *Appl. Phys. Lett.* 70 (1997) 652.
- [15] E.J. Meijer, M. Matters, P.T. Herwig, D.M. de Leeuw, T.M. Klapwijk, *Appl. Phys. Lett.* 76 (2000) 3433.
- [16] R. Widenhorn, L. Mundermann, A. Rest, E. Bodegom, *J. Appl. Phys.* 89 (2001) 8179.
- [17] J. Fortner, V.G. Karpov, M.L. Saboungi, *Appl. Phys. Lett.* 66 (1995) 997.
- [18] M. Kondo, Y. Chida, A. Matsuda, *J. Non-Crystalline Solids* 178 (1996) 198–200.
- [19] L. Pichon, A. Mercha, J.M. Routoure, R. Carin, O. Bonnaud, T. Mohammed-Brahim, *Thin Solid Films* 427 (2003) 350.
- [20] H. Overhof, P. Thomas, *Electronic Transport in Hydrogenated Amorphous Semiconductors*, Springer, Berlin, 1989.
- [21] G. Boisvert, L.J. Lewis, A. Yelon, *Phys. Rev. Lett.* 75 (1995) 469.
- [22] A. Yelon, B. Movaghar, *Phys. Rev. Lett.* 65 (1990) 618.
- [23] R. Widenhorn, A. Rest, E. Bodegom, *J. Appl. Phys.* 91 (2002) 6524.
- [24] I.I. Fishchuk, A.K. Kadashchuk, J. Genoe, Mujeeb Ullah, H. Sitter, Th.B. Singh, N.S. Sariciftci, H. Bässler, *Phys. Rev. B* 81 (2010) 045202.
- [25] R. Rawcliffe, D.D.C. Bradley, A.J. Campbell, *Proc. SPIE* 5217 (2003) 25.
- [26] R. Rawcliffe, D.D.C. Bradley, A.J. Campbell, *Proc. SPIE* 5519 (2004) 89.
- [27] J. Reynaert, V.I. Arkhipov, J. Genoe, G. Borghs, P. Heremans, *Mater. Res. Soc. Symp. Proc.* 846 (2005) DD6.8.1.
- [28] M. Kotani, K. Kakinuma, M. Yoshimura, K. Ishii, S. Yamazaki, T. Kobori, H. Okuyama, H. Kobayashi, H. Tada, *Chem. Phys.* 325 (2006) 160.
- [29] C. Tanase, E.J. Meijer, P.W.M. Blom, D.M. de Leeuw, *Phys. Rev. Lett.* 91 (2003) 216601.
- [30] L. Li, G. Mellera, H. Kosina, *Synth. Met.* 157 (2007) 243.
- [31] A.J. Mozer, G. Dennler, N.S. Sariciftci, M. Westerling, A. Pivrikas, R. Osterbacka, G. Juška, *Phys. Rev. B* 72 (2005) 035217.
- [32] A.J. Mozer, N.S. Sariciftci, A. Pivrikas, R. Osterbacka, G. Juška, L. Brassat, H. Bässler, *Phys. Rev. B* 71 (2005) 035214.
- [33] G. Juska, K. Arlauskas, M. Viliunas, J. Kocka, *Phys. Rev. Lett.* 84 (2000) 4946.
- [34] A. Pivrikas, R. Osterbacka, G. Juska, K. Arlauskas, H. Stubb, *Synth. Met.* 155 (2005) 242.
- [35] H. Sitter, T. Nguyen Manh, D. Stifter, *J. Cryst. Growth* 174 (1997) 828.
- [36] M. Shtein, J. Mapel, J.B. Benziger, S.R. Forrest, *Appl. Phys. Lett.* 81 (2002) 268.
- [37] C. Tanase, E.J. Meijer, P.W.M. Blom, D.M. de Leeuw, *Org. Electron.* 4 (2003) 33.
- [38] Mujeeb Ullah, D.M. Taylor, R. Schwödiauer, H. Sitter, S. Bauer, N.S. Sariciftci, Th.B. Singh, *J. Appl. Phys.* 106 (2009) 114505.
- [39] A. Palmaerts, L. Lutsen, T.J. Cleij, D. Vanderzande, A. Pivrikas, H. Neugebauer, N.S. Sariciftci, *Polymer* 50 (2009) 5007.
- [40] R. Osterbacka, A. Pivrikas, G. Juska, K. Genevicius, K. Arlauskas, H. Stubb, *Current Appl. Phys.* 4 (2004) 534.
- [41] H. Bässler, *Phys. Stat. Sol. B* 175 (1993) 15.
- [42] Mujeeb Ullah, T.B. Singh, H. Sitter, N.S. Sariciftci, *Appl. Phys. A: Mater. Sci. Process* 97 (2009) 521.
- [43] Mujeeb Ullah, I.I. Fishchuk, A.K. Kadashchuk, P. Stadler, A. Pivrikas, C. Simbrunner, V.N. Poroshin, N.S. Sariciftci, H. Sitter, *APL* 96 (2010) 213306.